

# Radon variation measurements at the Yangyang underground laboratory

C. Ha,<sup>1</sup> W. G. Kang,<sup>2</sup> J. Kim,<sup>1</sup> K. W. Kim,<sup>2</sup> S. K. Kim,<sup>3</sup> Y. D. Kim,<sup>2,4</sup>  
H. S. Lee,<sup>2,4</sup> M. H. Lee,<sup>2,4</sup> M. J. Lee,<sup>5</sup> Y. J. Lee,<sup>1</sup> and Y. Jeong<sup>1</sup>

<sup>1</sup>*Department of Physics, Chung-Ang University, Seoul 06974, Republic of Korea*

<sup>2</sup>*Center for Underground Physics, Institute for Basic Science (IBS), Daejeon 34126, Republic of Korea*

<sup>3</sup>*Department of Physics and Astronomy, Seoul National University, Seoul 08826, Republic of Korea*

<sup>4</sup>*IBS school, University of Science and Technology (UST), Daejeon 34113, Republic of Korea*

<sup>5</sup>*Department of Physics, Sungkyunkwan University, Suwon 16419, Republic of Korea*

(Dated: September 5, 2022)

From October 2004 to May 2022, the concentration of radon in the air was measured at a depth of 700 m in the Yangyang underground laboratory. The average rates in the two experimental areas, called A6 and A5, were measured as  $53.4 \pm 0.2$  Bq/m<sup>3</sup> and  $33.5 \pm 0.1$  Bq/m<sup>3</sup>, respectively. The lower rate in the A5 area was caused by the improved temperature control and ventilation. In particular, these radon rates are correlated to the local temperature of the area, with a correlation coefficient  $r = 0.22$ . Therefore, the radon rates displayed a seasonal variation, because the local temperature driven by the overground season influences air ventilation in the experimental areas. A cosine fit on the annual residual rates exhibited the maximum amplitude on August  $31 \pm 6$  d every year.

## INTRODUCTION

The materials composing our universe are predominantly radiationless dark components, but their nature is not adequately understood. Based on astrophysical observations, we indirectly realized that 26% of all energy is formed by dark matter [1]. Theoretically, the components of dark matter have been modeled as particles beyond the Standard Model [2, 3], wherein a weakly interacting massive particle (WIMP) is one of the strongest candidates [4]. In particular, the search for a WIMP is being experimentally conducted through several approaches [5–7], one of which involves the measurement of the energy deposited from the nuclear recoil at the instant a WIMP interacts in a target medium.

Thus far, no direct measurement of a WIMP–nucleus interaction has been recorded, except for DAMA experiments that record annual modulations of residual events in a background rate that can be regarded as a result of the Earth’s motion in the WIMP-present galactic halos [8, 9]. However, the annual modulation signal cannot be explained by known background sources. For a potential explanation, muon-induced processes and radon concentrations in the air have been suggested and studied [10–14]. Among various possibilities, radon monitoring is essential for correlation studies with annual modulation analysis data. In principle, radon is produced as a daughter nuclei decay product from the radioactive material present in the tunnel. Specifically, the rock samples containing uranium and thorium act as the primary sources of radon. If radon decays into its daughter isotopes, several gamma rays are produced and can contribute to the background spectrum of the dark matter data.

The Yangyang underground laboratory hosts two dark matter experiments and one neutrinoless double-beta decay experiment, and since 2004, we have collected under-

ground radon data with environmental parameters using custom-design and commercially available detectors. In this study, we analyzed a long-term radon level variation based on these measurements.

## MATERIALS AND METHODS

### Experimental sites at Yangyang underground laboratory

The Yangyang underground laboratory (Y2L) is located adjacent to the underground generator of the Yangyang pumped water plant in east Korea. The plant contains the main access tunnel with auxiliary tunnels, named as A5 and A6, housing the experimental facilities. Fresh air from the surface enters the tunnels through the main ramp way and is pumped out via a separate duct. Throughout the year, the temperature inside the tunnel is maintained between 22 °C and 25 °C, and the relative humidity in the areas surrounding the laboratory is in the ranges of 60–70%. The minimum granite overburden in these areas is 700 m and the cosmic-ray muon fluxes at A5 and A6 (two are situated 300 m apart horizontally) were measured as  $3.795 \pm 0.110 \times 10^{-7}$  s<sup>-1</sup> cm<sup>-2</sup> [15, 16] and  $4.4 \pm 0.3 \times 10^{-7}$  s<sup>-1</sup> cm<sup>-2</sup> [17], respectively. The subterranean rock is primarily composed of gneiss that contains 2.1 ppm and 13.0 ppm of uranium and thorium, respectively, measured by the inductively coupled plasma mass spectrometry [18].

The Korea Invisible Mass Search (KIMS) experiment [19] in the A6 tunnel has operated a CsI (Tl) crystal array to search dark matter search for more than 15 years, and it is currently conducting R&D activities related to the development of ultralow-background crystals. The COSINE-100 experiment [20, 21] is operated using NaI(Tl) crystals in the A5 experimental space.

Furthermore, additional experiments such as a neutrino-less double-beta decay experiment called the advanced molybdenum-based rare process experiment (AMoRE-I) [22] and high-purity Germanium array (HPGe) [23] are operated in the A5 tunnel in separate rooms. Moreover, a radon reduction system (RRS) is equipped in the A5 area, and it supplies radon-filtered air to each experimental room when required. If the RRS provides radon-reduced air to the rooms, the measured radon level is broadly 10–100 times less than that of the tunnel air. As the A6 tunnel area is separated from the main tunnel by doors, the presiding air flow is minimal. In contrast, the entrance of the A5 tunnel is opened in all instances and the tunnel is equipped with its own air exhaust system that provides relatively improved air circulation. The Y2L drawing with the experimental areas indicated is presented in Fig. 1.

The COSINE-100 experiment is housed in an environmentally regulated room with controlled humidity and temperature. The detection room houses an area of 44 m<sup>2</sup> and a height of 4 m. In particular, the air control system maintains the room temperature at  $23.5 \pm 0.1$  °C and relative humidity at  $37 \pm 1$  %. The air in the room is continuously circulated through a HEPA filter, and the number of dust particles larger than 0.5  $\mu\text{m}$  is maintained below 1500 per cubic foot. These environmental parameters in the experimental room and in the tunnel are monitored online. The details of experimental control are described in [24].

### Radon Counter Setup

Since 2004, the custom-design radon detector measured the radon rate at the A6 KIMS detector room, and in 2011, this detector was replaced with a commercially available detector from DurrIDGE company (RAD7-1). In 2016, the RAD7-1 detector was moved to the COSINE-100 detector room, and it has been functioning hence. The same model counter (RAD7-2) was installed in the HPGe detector room in 2016. In RAD7, the silicon diode sensor is located at the center of the drift chamber, wherein an electric field is applied. If a <sup>222</sup>Rn nucleus decays in the middle of the chamber, it becomes a positively charged <sup>218</sup>Po ion that adheres to the diode’s sensitive area, following the electric field. After several minutes, this <sup>218</sup>Po decays into a <sup>214</sup>Pb nuclei and an alpha particle. Thus, the alpha particle deposits energy at a rate that reflects the mother <sup>222</sup>Rn isotope activity. The total radon levels are measured every two hours against room air and the recorded data are transmitted to a slow monitoring server, as displayed in Fig. 2.

These RAD7 detectors have been cross-measured at various locations in the overground labs and cross-checked with a separate custom-made detector, includ-

ing a commercial ion chamber detector (RadonEye [25]). All these tests yielded consistent results and the RAD7 detectors did not exhibit any abnormal behavior as long as the desiccants were regularly replaced to maintain the humidity inside the chamber.

### Data collection

With 4762 days of the total operational period between October 2004 and May 2022, the radon data were acquired in three distinct periods at the Y2L. At the A6 lab, The KIMS custom-made detector operated for 5 years until October 2009. The data presented herein are reported in Ref. [18], which applies a prescale factor of 10. After 16 months of no measurements, the RAD7-1 detector was installed at the same location. In September 2016, the RAD7-1 detector was moved to the A5 COSINE-100 room for data acquisition. In a similar timeframe, we operated another detector—RAD7-2 in the HPGe room at A5. Overall, these RAD7 detectors were continuously running with a short dead time that was primarily caused by the power outage in the tunnel. Herein, the physics analyses were performed based on the entire acquired data. The measurement locations, detector type, periods, and measured radon rates are summarized in Table I.

The radon rate (in Becquerel per cubic meter) is displayed in Figure 2 as a function of the date for all acquired data. In particular, three distinct measurements were acquired broadly in 5 years and are correspondingly color-coded. As listed in Table I, the average rates were at the level of 1 pCi/L (=37 Bq/m<sup>3</sup>), which is relatively low compared to other underground lab measurements [26, 27]. The long-term structure in the rate variation primarily results from the air circulation in the tunnel. From late 2008 to late 2010, the temporal variations executed in the A6 ventilation system allowed airflow inside the tunnel area, which caused lower activity in that period. The fundamental reason for the occasional short-term spikes in the data is because the detector is in relatively humid condition owing to the poor maintenance of the chamber air desiccant. The detector specified 5 % accuracy in normal humidity levels [28]. In the case of supplying radon-reduced air into one of the experimental rooms, the radon level is typically reduced to a few Bq/m<sup>3</sup> (RAD7 detection limit is at 4 Bq/m<sup>3</sup>). The distributions of radon activities were comparatively analyzed for each measurement, as illustrated in Fig. 3.

## RESULTS

With the acquired data, we performed analyses among the measurements in terms of their rates and function of time. The radon rate measured at A5 was  $33.5 \pm 0.1$

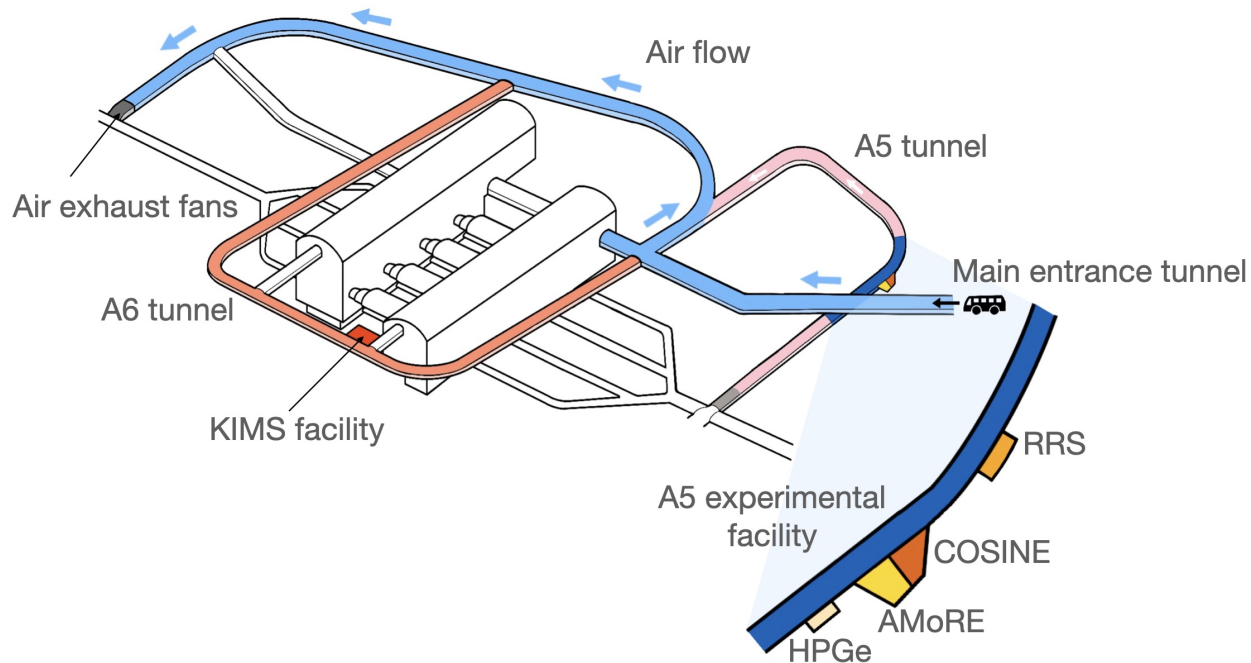


FIG. 1. Y2L map. Experimental areas are accessed by cars through the main entrance. Air is exhausted by fans at the end of the main tunnel, and therefore, fresh air enters in a single direction. KIMS experiment is located in the A6 tunnel, whereas the newer facilities are situated in the A5 tunnel, hosting COSINE-100, AMoRE-I, and HPGe experiments. A5 and A6 are situated 300 m away horizontally, and A5 is approximately 50 m deeper than A6.

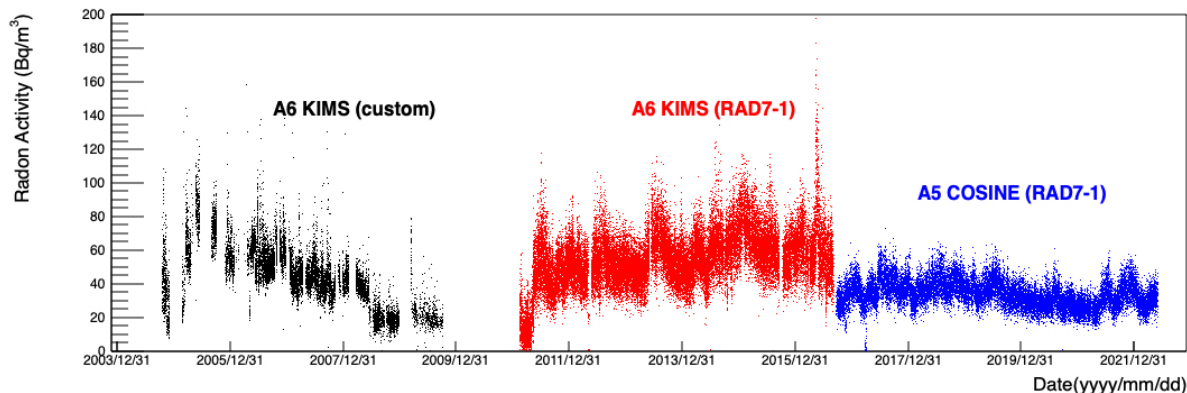


FIG. 2. Radon concentration in Y2L between 2004 and 2022 was measured in two distinct experimental areas. At the KIMS laboratory, the custom detector measurements were performed from October 2004 to October 2009 (black), whereas the RAD7-1 measurements were recorded between February 2011 and September 2016 (red). The COSINE-100 measurement data were acquired from September 2016 to May 2022 (blue) with the same RAD7-1 counter. Note that the HPGe data are not displayed for improved visibility.

$\text{Bq/m}^3$ , which was less than that of A6 by 37%. The reduction was primarily caused by the ventilation condition in the tunnel. The A6 tunnel is a both-end closed space with minimal airflow, whereas the entrance of the A5 tunnel is one-end opened, and therefore, the air circulation

in the A5 tunnel is superior to that in A5. Additionally, the COSINE-100 room from which air is sampled by the RAD7-1 detector is equipped with a temperature and humidity controller along with dust filters. Therefore, the variance of the measurements is  $7.9 \pm 0.1 \text{ Bq/m}^3$ , which is

TABLE I. Detector and locations. All acquired Y2L radon data. KIMS-Custom measurement data presented with prescale factor of 10, and radon value included systematic uncertainties, whereas those of other RRS measurements presented only statistical uncertainties. Notably, radon level in HPGe measurement represents values if the RRS air is not supplied (\*).

Experiment (Location)	Counter Type	Period	Radon(Bq/m <sup>3</sup> )	Live days (%)
KIMS (A6)	Custom	2004.10.18–2009.10.05	44.4 ± 18.1	847(46.7)
KIMS (A6)	RAD7-1	2011.02.14–2016.09.01	53.4 ± 0.2	1872(92.3)
COSINE-100(A5)	RAD7-1	2016.09.23–2022.05.27	33.5 ± 0.1	2043(98.6)
HPGe (A5)	RAD7-2	2016.09.28–2022.05.27	35.2 ± 0.2*	–

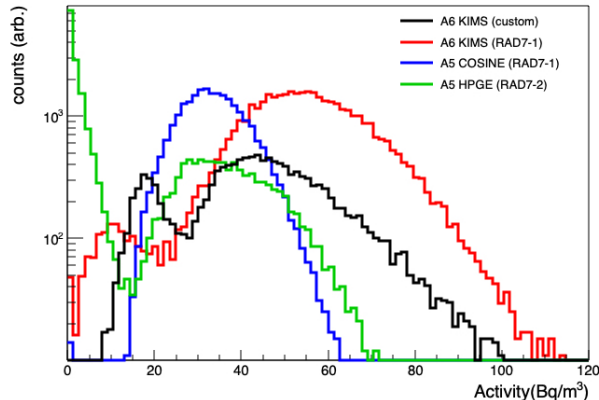


FIG. 3. Radon activities in Y2L detector rooms. Radon data were compared among three distinct Y2L experimental areas. Gaussian fit overlaid on A6 KIMS lab measurement (red) displays  $53.4 \pm 0.2$  Bq/m<sup>3</sup> and  $13.9 \pm 0.3$  Bq/m<sup>3</sup> for mean and sigma, respectively, whereas the measurement on the A5 COSINE-100 laboratory (blue) depicts  $33.5 \pm 0.1$  Bq/m<sup>3</sup> and  $7.9 \pm 0.1$  Bq/m<sup>3</sup>. The measurement on the A5 HPGe room (green) exhibits two populations depending on the radon-reduced air supply.

less than  $13.9 \pm 0.3$  Bq/m<sup>3</sup> for A6. The long-term variations for A5 measurements have been investigated by correlating the rates with tunnel temperature. The radon residual rate has been evaluated based on the annual average values and those fitted with a sinusoidal function to understand any periodic nature.

The rates measured at the A5 COSINE-100 and HPGe rooms were compared to each other as well as with the temperature in the A5 tunnel. As stated earlier, the two experimental rooms are separated by a distance of approximately 35 m. If RRS is non-operational, the comparative analysis of the variations in radon measurements reveal a strong correlation, as depicted in Fig. 4.

The tunnel temperature varies annually with the temperature of the local province, because the power plant company operates air circulation fans at the end of the main tunnel all throughout the year by drawing in outside air. The temperature measured at the A5 tunnel varied between 22 °C and 25 °C (Fig. 4). In the Yangyang

province, the annual average temperature is 11.8 °C, and on average, the minimum is  $-2.2$  °C in January and the maximum is 24.3 °C during August.

The radon rates measured at the COSINE-100 and HPGe rooms are compared with the temperature inside the A5 tunnel in Figure 5. A5 COSINE-100 radon measurement is correlated with the tunnel temperature and the correlation coefficient  $r = 0.22$ , and the slope of the linear fit on the data was measured as 64%.

For an annual variation analysis, we applied an additional selection criterion from all the acquired KIMS and COSINE-100 radon data. This eliminated all the data prior to 2011/05/11, with knowledge of the irregular condition in the ventilation of the A6 tunnel and the occasional detector fault indicated from the incomplete data. The combined data period is from 2011/05/11 to 2022/05/27 (4034 d) and the final analysis sample contains 3822 live days, which is 95% of this period. We treat the RAD7 reported two-hour measurement as a single counting. Each daily measurement is a statistical average of the two-hour measurements on that day, and it was further combined as an eight-day bin.

Initially, we evaluated an annual average using a period of 365.25 d from the beginning of a year. After subtracting the average values, the residual spectra for each year were obtained and combined for the entire analysis period. Thereafter, we used a cosine fit,

$$f(t) = A \cos\left(\frac{2\pi}{365.25}(t - t_0)\right) \quad (1)$$

on this residual data. In Eq. 1, the period was set at 1 year and we fit two parameters, namely, amplitude  $A$  and phase  $t_0$ . The best-fit phase at a positive maximum amplitude was derived at  $60.6 \pm 5.6$  d, which approximately corresponds to August 31 ± 6 d every year. The residual radon data and the best fit are displayed in Fig. 6.

## DISCUSSION

We reviewed a phase for the A5 temperature annual variation fitted considering the same Eq. 1. This yielded the peak amplitude-phase of  $58.4 \pm 5.2$  d, which was consistent with the best-fit phase of the radon variations.

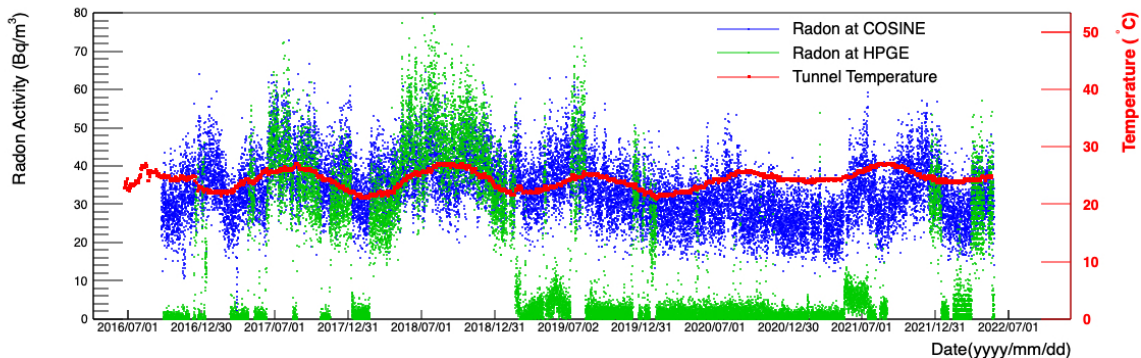


FIG. 4. Radon rates in various detector rooms. HPGe radon measurement (green) and that of COSINE-100 (blue) have been compared. The two detector rooms are separated by a distance of approximately 35 m. The HPGe detector (RAD7-2) reflects the same type from the same company as the COSINE-100 RAD7 detector (RAD7-1). The occasional reduction in the radon level at HPGe was caused by the radon-free air flushing in the room by the RRS system. In case the RRS is switched off, two detector room measurements could be appropriately correlated to each other, implying that the fundamental radon activity is not caused by the local room effect.

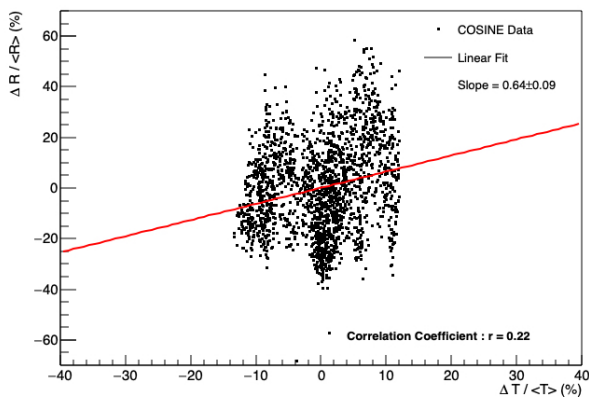


FIG. 5. Relative radon fraction versus temperature variation fraction. The ratio of radon rate variation to the average rate for COSINE-100 room measurements by RAD7-1 is plotted with the ratio of temperature variations to average temperature. Linear fit exhibits a slope of  $0.64 \pm 0.09$  and the Pearson correlation coefficient is evaluated as  $r = 0.22$ .

Thus, we concluded that the observed radon modulation results from the air ventilation, which is driven by the temperature variations in the tunnel. If the main tunnel draws warm air from outside, e.g., in summer, the air circulations in the branch tunnels such as A5 and A6 deteriorate because of the weak temperature gradient created between the main and branch tunnels. Conversely, in winter, the warm air in the branch tunnels readily emerges into the flow of the main tunnel owing to the larger temperature gradient.

Compared to the phase of DAMA/LIBRA (June 1<sup>st</sup>), this value lags by more than two months. In contrast,

this varies roughly by a month from the COSINE-100 muon measurement (June 27<sup>th</sup>). Overall, the results of the COSINE-100 and ANAIS annual modulation are statistics-limited at the moment, and therefore, they cannot be directly compared for obtaining meaningful insights.

The radon concentration in the air has been measured over the past 18 years in the Y2L laboratory. The average rate is  $53.4 \pm 0.2$  Bq/m<sup>3</sup> at the A6 laboratory and  $33.5 \pm 0.1$  Bq/m<sup>3</sup> at the A5 laboratory, which has been reduced by 37% in the newer lab equipped with temperature and ventilation control. In this analytical study, we determined that the radon rate is correlated to the tunnel temperature. The COSINE-100 room radon rate and tunnel temperature are correlated with the coefficient of  $r=0.22$ . With the selected data, the yearly residual data were fit with a cosine function and the phase was derived at August  $31 \pm 6$  d, which coincides with the temperature variation in the same tunnel. Overall, this is the longest measurement of the low-radon rate in underground laboratories.

## ACKNOWLEDGMENTS

We thank the Korea Hydro and Nuclear Power (KHNP) Company for providing the underground laboratory space at Yangyang. This research was supported by the Chung-Ang University Graduate Research Scholarship in 2022 and by the National Research Foundation of Korea (NRF) grant funded by the Korean government (MSIT) (No. 2021R1A2C1013761).

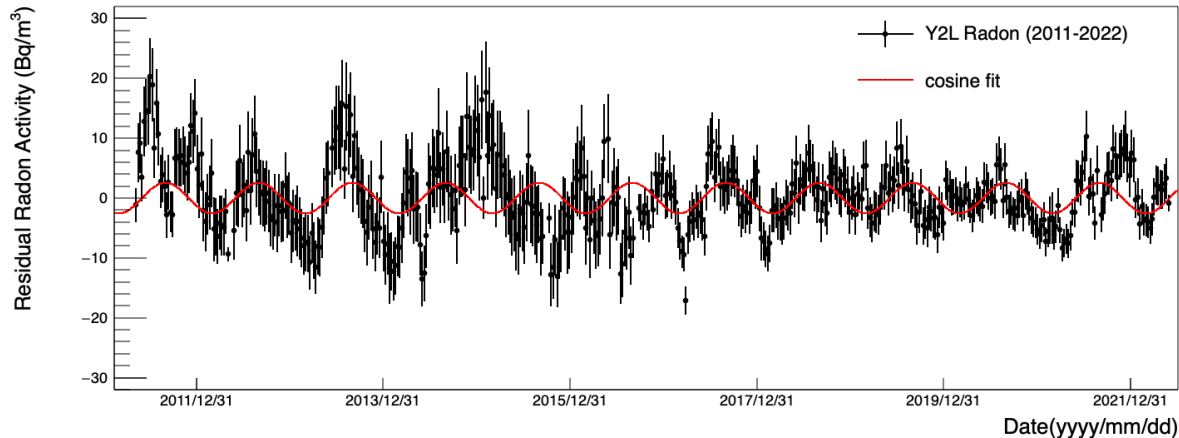


FIG. 6. Residual radon rate as a function of time. The residual rate obtained from KIMS and COSINE-100 data is fitted with the cosine function. The period is set at 365.25 d and the amplitude and phase of function have been freely floated. The best-fit phase at a positive maximum amplitude was evaluated as  $60.6 \pm 5.6$  d, which approximately corresponded to August  $31 \pm 6$  d every year.

- 
- [1] P. A. R. Ade *et al.* (Planck Collaboration), *Astron. Astrophys.* **594**, A13 (2016).
- [2] F. Zwicky, *ApJ* **86**, 217 (1937).
- [3] M. Tanabashi *et al.* (Particle Data Group), *Phys. Rev. D* **98**, 030001 (2018).
- [4] B. W. Lee and S. Weinberg, *Phys. Rev. Lett.* **39**, 165 (1977).
- [5] M. Schumann, *J. Phys. G* **46**, 103003 (2019), arXiv:1903.03026 [astro-ph.CO].
- [6] J. M. Gaskins, *Contemp. Phys.* **57**, 496 (2016), arXiv:1604.00014 [astro-ph.HE].
- [7] F. Kahlhoefer, *Int. J. Mod. Phys. A* **32**, 1730006 (2017), arXiv:1702.02430 [hep-ph].
- [8] R. Bernabei *et al.*, *Proceedings, 7th International Conference on New Frontiers in Physics (ICNFP 2018): Kolymbari, Crete, Greece, July 4-12, 2018*, *Universe* **4**, 116 (2018), arXiv:1805.10486 [hep-ex].
- [9] K. Freese, M. Lisanti, and C. Savage, *Rev. Mod. Phys.* **85**, 1561 (2013).
- [10] J. H. Davis, *Phys. Rev. Lett.* **113**, 081302 (2014).
- [11] K. Blum, (2011), arXiv:1110.0857.
- [12] A. Tiwari, C. Zhang, D. M. Mei, and P. Cushman, *Phys. Rev. C* **96**, 044609 (2017), [Erratum: *Phys. Rev. C* **98**, 019901 (2018)], arXiv:1706.00100 [hep-ex].
- [13] P. Adamson *et al.* (MINOS), *Phys. Rev. D* **87**, 032005 (2013), arXiv:1212.1776 [hep-ex].
- [14] D. N. McKinsey, (2018), arXiv:1803.10110 [hep-ex].
- [15] H. Prihtiadi *et al.* (COSINE-100 Collaboration), *JINST* **13**, T02007 (2018).
- [16] H. Prihtiadi *et al.* (COSINE-100), *JCAP* **02**, 013 (2021), arXiv:2005.13672 [physics.ins-det].
- [17] J. Zhu *et al.* (KIMS), *High Energy Physics and Nuclear Physics* **29**, 721 (2005).
- [18] M. Lee *et al.* (KIMS Collaboration), *J. Korean Phys. Soc.* **57**, 713 (2011).
- [19] H. S. Lee *et al.* (Kims), *Phys. Lett. B* **633**, 201 (2006), arXiv:astro-ph/0509080.
- [20] G. Adhikari *et al.*, *Eur. Phys. J. C* **78**, 107 (2018), arXiv:1710.05299 [physics.ins-det].
- [21] G. Adhikari *et al.*, *Nature* **564**, 83 (2018), [Erratum: *Nature* **566**, E2 (2019)], arXiv:1906.01791 [astro-ph.IM].
- [22] V. Alenkov *et al.*, *Eur. Phys. J. C* **79**, 791 (2019), arXiv:1903.09483 [hep-ex].
- [23] D. S. Leonard *et al.*, *Nucl. Instrum. Meth. A* **989**, 164954 (2021), arXiv:2009.00483 [physics.ins-det].
- [24] H. Kim *et al.* (COSINE-100), *JINST* **17**, T01001 (2022), arXiv:2107.07655 [physics.ins-det].
- [25] “Radoneye rd200 radon detector,” <http://radoneye.com/> (2022).
- [26] G. Pronost, M. Ikeda, T. Nakamura, H. Sekiya, and S. Tasaka, *PTEP* **2018**, 093H01 (2018), arXiv:1807.11142 [physics.ins-det].
- [27] C. Liu, H. Ma, Z. Zeng, J. Cheng, J. Li, and H. Zhang, (2018), arXiv:1806.06567 [physics.ins-det].
- [28] “DurrIDGE rad7 radon detector,” <https://durrIDGE.com/products/rad7-radon-detector> (2022).